Journal of Chromatography A, 1218 (2011) 4537–4544

Contents lists available at ScienceDirect

Journal of Chromatography A

journal homepage: www.elsevier.com/locate/chroma

Improved enantiomer resolution and quantification of free D-amino acids in serum and urine by comprehensive two-dimensional gas chromatography–time-of-flight mass spectrometry

Magdalena C. Waldhier[a,*,1], Martin F. Almstetter[a,1], Nadine Nürnberger[a], Michael A. Gruber[b], Katja Dettmer[a], Peter J. Oefner[a]

[a] Institute of Functional Genomics, University of Regensburg, Josef-Engert-Str. 9, 93053 Regensburg, Germany
[b] Department of Anesthesiology, University Hospital Regensburg, Franz-Josef-Strauss-Allee 11, 93053 Regensburg, Germany

ARTICLE INFO

Article history:
Received 14 November 2010
Received in revised form 17 March 2011
Accepted 10 May 2011
Available online 19 May 2011

Keywords:
Enantioselective analysis
GC × GC–TOFMS
Methyl chloroformate
Metabolomics
Urine
Serum

ABSTRACT

The potential of comprehensive two-dimensional gas chromatography–time-of-flight mass spectrometry (GC × GC–TOFMS) in the quantitative analysis of amino acid enantiomers (AAEs) as their methyl chloroformate (MCF) derivatives in physiological fluids was investigated. Of the two column sets tested, the combination of an Rt-γDEXsa chiral column with a polar ZB-AAA column provided superior selectivity. Twenty AAEs were baseline resolved including L-Leu and D-Ile, which had failed separation by one-dimensional chiral GC–quadrupole-MS (GC–qMS). Lower limits of quantification (LLOQ) were in the range of 0.03–2 μM. Reproducibility of the analysis of a serum specimen in octaplicate ranged from 1.3 to 16.6%. The GC × GC–TOFMS method was validated by analyzing AAEs in 48 urine and 43 serum specimens, respectively, and by comparing the results with data obtained by a previously validated GC–qMS method. Mean recoveries ranged from 78.4% for D-Leu to 116.4% for D-Pro in urine and 72.2% for L-Thr to 129.4% for L-Ile in serum. The method was applied to the comparison of AAE serum levels in patients suffering from liver cirrhosis to a control group. Significantly increased D-AA concentrations were found for the patient group, whereas L-AA levels were slightly decreased.

1. Introduction

The enantioselective analysis of amino acids is attracting increasing interest due to a better understanding of the biological relevance of D-AAs. D-AAs are found in bacteria, mammalians, plants, and food [1–7]. In humans, D-AAs originate primarily from bacterial metabolism and food intake [3–5,8]. D-AA elimination proceeds mainly by renal excretion. Further, enzymes catalyzing D-AA decomposition, such as D-AA oxidase and D-aspartate oxidase, have been found in brain, liver and kidney [9,10]. AAE separation and quantification relies primarily on chromatographic and electrophoretic strategies [11]. Recently, we developed a GC–qMS method based on pre-column derivatization with methanol/methyl chloroformate (MeOH/MCF) and separation on a γ-cyclodextrin (γ-CD) based column (Rt-γDEXsa) for the quantitative analysis of proteinogenic AAEs. Twelve out of the twenty proteinogenic AAs eluted from the Rt-γDEXsa column including Ala, Gly, Val, Leu, Ile, Pro, Thr, Asp, Ser, Met, Asn, and Phe. For each corresponding enantiomer pair, baseline separation was achieved except for the Phe enantiomers [12]. However, D-Ile/L-Leu, L-Thr/L-Asp, and L-Ser/D-Met, respectively, were not baseline separated from each other. The use of unique *m/z* ions allowed the quantification of coeluting L-Thr and L-Asp. Quantification was not possible for D-Ile and L-Leu, which are structural isomers forming identical fragment ions and, therefore, necessitate baseline separation [12]. Furthermore, quantification was impaired for L-Ser and D-Met, because they were incompletely resolved and no unique *m/z* ion could be found for L-Ser. Consequently, improved resolution is needed for the GC–MS analysis of AAEs. This may be achieved by comprehensive two-dimensional gas chromatography–time-of-flight mass spectrometry (GC × GC–TOFMS), which provides a multiplicative increase in peak capacity as well as improved resolution and detection sensitivity over conventional GC–MS methods [13,14].

Junge et al. were the first to apply GC × GC to the separation of AAEs as their N-trifluoroacetyl methyl esters in samples of beer by coupling a Chirasil-L-Val column with a low-polarity column in the second-dimension [15]. The present study expands the scope of GC × GC-based AAE analysis by applying a combination of an Rt-γDEXsa chiral first-dimension column with an RTx-1701 or a ZB-AAA column as second-dimension column not only to the sepa-

* Corresponding author. Tel.: +49 (0) 9419435006; fax: +49 (0) 9419435020.
E-mail address: magdalena.waldhier@klinik.uni-regensburg.de (M.C. Waldhier).
[1] These authors contributed equally to this work and therefore should be considered equal first authors.

0021-9673/$ – see front matter © 2011 Elsevier B.V. All rights reserved.
doi:10.1016/j.chroma.2011.05.039

ration but also quantitative measurement of AAEs in physiological fluids after off-line pre-column derivatization with MeOH/MCF. The performance of the superior column combination was then compared to that of the previously published GC–qMS method [12].

2. Experimental

2.1. Materials

Isooctane, pyridine, MCF, D-norvaline, D-lactic acid, all solids of L and D configured AAs, as well as racemates of proteinogenic AAs, were purchased from Sigma–Aldrich (Taufkirchen, Germany). Aqueous stock solutions were prepared from the L- and D-AA solids at concentrations of 11–60 mM. Racemic stock solutions contained enantiomers in the range of 7.0–46.5 mM. From these solutions a master mixture was prepared containing Gly and all enantiomers that elute from the Rt-γDEXsa column as MeOH/MCF derivatives at a concentration of 1 mM each. The [U-^{13}C, U-^{15}N] cell free amino acid mix was obtained from Euriso-top (Saint-Aubin Cedex, France). The combined D + L-concentrations of the 20 proteinogenic AAs contained in the mixture ranged between 0.37 and 2.58 mM, but no information on D-AA ratios was available. Methanol (LC–MS grade) and chloroform (HPLC grade) were purchased from Fisher Scientific GmbH (Ulm, Germany).

2.2. Biological samples

A set of 48 urine and 43 serum specimens, which had been collected from patients before and after curative stem cell transplantation for non-malignant and malignant disorders of the immunohematopoietic system, was used to validate the GC × GC–TOFMS method with the Rt-γDEXsa/ZB-AAA column set by comparing determined AAE amounts with the results obtained by the GC–qMS method [12]. Urine samples were not treated with preservatives but were frozen at −20 °C as quickly as possible after sampling to avoid bacterial growth. Further, 25 serum specimens from patients with liver cirrhosis and 16 control sera were analyzed by the validated method to demonstrate relevance for medical diagnostics. At the time of blood drawing, none of the patients had been treated with peptide antibiotics or other drugs that might affect D-AA serum levels. Serum specimens were stored at −80 °C. Specimens were provided by collaborators at the University Hospital of Regensburg with approval from the institutional review board.

2.3. Instrumentation

The LECO (St. Joseph, MI) Pegasus 4D GC × GC–TOFMS instrument comprised an Agilent Technologies Model 6890 GC, a dual-stage, quad-jet thermal modulator, a secondary oven coupled to a fast acquisition TOFMS providing unit mass resolution, a PTV injector (Gerstel, Muehlheim, Germany), and a MPS-2 Prepstation sample robot (Gerstel). The robot was equipped with a 10 μL-syringe for sample injection. Between injections the syringe was washed with 5 volumes of isooctane. Samples were kept in a cooled tray at 5 °C. An Rt-γDEXsa column (30 m × 0.25 mm ID, 0.25 μm film thickness) from Restek (GmbH, Bad Homburg, Germany) protected by a 5 m × 0.25 mm ID fused silica deactivated guard column (Agilent Technologies, Palo Alto, CA, USA) was used as the first-dimension column, while an RTx-1701 (2 m × 0.1 mm ID × 0.1 μm film thickness, Restek) or a ZB-AAA (2 m × 0.25 mm ID, 0.25 μm film thickness, Phenomenex Inc.) column served as the second-dimension column. A sample volume of 1.5 μL was injected in splitless mode with the temperature of the PTV Injector set at 50 °C for 0.5 min and then ramped at 12 °C/s to 250 °C. A chemically inert Siltek liner from Gerstel was used. The helium flow-rate was set at 1.9 mL/min (constant flow). Modulation was accomplished every 4 s during GC × GC analysis and modulator hot pulse time was 0.6 s. Mass spectra were acquired from 40 to 600 *m/z* at a rate of 200 spectra/s. For 1D GC–TOFMS analysis the modulator was turned off and mass spectra were collected at 50 spectra/s. The solvent delay was kept at 19 min. Transfer-line temperature was held at 260 °C. The ion source was operated at 200 °C and −70 eV. A positive offset of 5 °C was used for the second-dimension column and a 15 °C offset relative to the first-dimension column for the modulator.

2.4. Sample preparation

Derivatization of AAEs with MeOH/MCF was performed as recently reported with subsequent extraction of derivatives into 300 μL of chloroform [12]. Sample and standard solution aliquots of 150 μL and 20 μL of internal standard mix were used for quantitative analysis. For preliminary experiments, 100 μL of a master mixture of AAEs was derivatized.

2.5. GC parameters

Temperature programs employed are listed in Table 1. Method A was used for the Rt-γDEXsa/RTx-1701 column set, while methods B and C were applied to the Rt-γDEXsa/ZB-AAA column set.

2.6. Quantification and method validation

Calibration was performed with the Rtγ-DEXsa/ZB-AAA column set using a 16 point-serial dilution of the master mixture. It contained all AAs, whose elution from the RTγ-DEXsa column as MeOH/MCF-derivatives could be detected, over a concentration range of 31 nM to 1 mM each. The applied internal standard solution contained 20 uniformly ^{13}C-, ^{15}N-labeled AA types at different concentrations between 0.37 and 2.58 mM. As the labeled AAs had been gained from algae, they were present in the mix at their naturally occurring ratios in algae. Most D-AAs were detected in the labeled mix but their abundance was too low (<3.4% of the respective L-AA area) to be suitable as internal standards. Thus, the stable isotope-labeled L-enantiomers of Ala, Val, Leu, Ile, Pro, Thr, Asp, Ser, Met, Asn, and Phe were used to correct areas of the corresponding D- and L-AA in quantitative measurements. Correspondingly, stable isotope-labeled Gly, the only natural nonchiral AA, was used for correcting Gly area integrals. LLOQ was defined as the lowest concentration of the calibration with an accuracy of ±20% and a signal-to-noise ratio of at least 10:1. Eight aliquots of a human serum specimen were prepared and analyzed to test method reproducibility. Accuracy was checked by comparing results with those obtained by the recently validated GC–qMS method for AAE analysis [12]. Relative recoveries were determined for urine (n = 48)

Table 1
Optimized GC temperature programs for the column sets RT-γDEXsa/RTx-1701 (A) and RT-γDEXsa/ZB-AAA (B, C), respectively.

Method	Temperature program
A	70 °C (1 min) – 2 °C/min – 150 °C (10 min) –2 °C/min – 180 °C (25 min)
B	70 °C (1 min) – 4 °C/min – 150 °C (10 min) – 3 °C/min – 190 °C (15 min)
C	70 °C (1 min) – 2 °C/min – 130 °C (12.5 min) – 8 °C/min – 150 °C (4 min) – 4 °C/min – 190 °C (6 min)

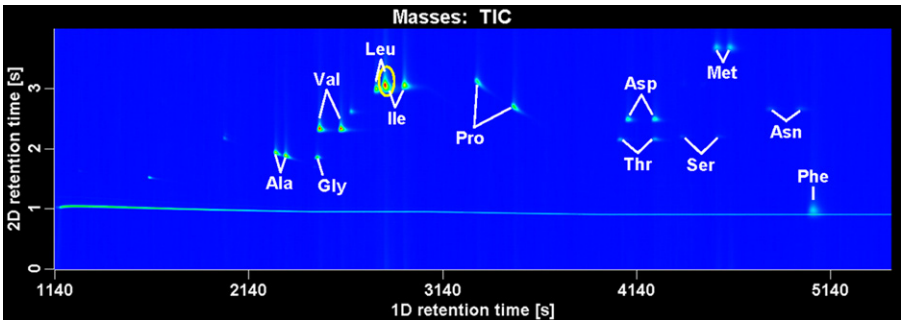

Fig. 1. Total ion current (TIC) 2D chromatogram of the master mixture using the Rt-γDEXsa/RTx-1701 column set and GC method A. D-Ile/L-Leu isomers are encircled.

and serum ($n = 43$) by dividing the enantiomer amount determined by GC × GC by the respective amount measured by chiral GC–qMS analysis and multiplying by 100. Mean recoveries as well as Pearson correlation coefficients were calculated. Additionally, Bland–Altman plots were generated, which display for each specimen analyzed the difference in concentration versus the mean of the concentrations determined by two methods and, therewith, assesses agreement between two methods [16–18]. Every Bland–Altman plot includes three horizontal lines that mark the mean difference and the upper and lower limits of agreement which are defined as mean difference ± 1.96 times SD of the difference. Since it takes too much space to show all Bland–Altman plots, the mean difference was divided by the averaged mean of all couples and multiplied by 100. These values were named 'mean deviation'.

2.7. Data analysis

Raw data were processed with the LECO ChromaTOF software version 3.34. Baseline correction, deconvolution and peak picking were performed. For identification, electron ionization (EI) spectra were compared to the EI spectra of the validated GC–qMS method [12].

3. Results and discussion

Initial experiments focused on the evaluation of two different column combinations for the GC × GC separation of MeOH/MCF derivatives of AAEs. In GC × GC the length of the second-dimension is kept short to allow the elution of analytes within one modulation period. Length of the first-dimension column, in contrast, is not limited. Therefore, the chiral Rt-γDEXsa column was always chosen as first-dimension stationary phase, as the resolution of enantiomers improves with increasing length of the chiral column. Secondly, the Rt-γDEXsa phase reacted sensitive to high temperatures, resulting in reduced enantioselectivity and accelerated column degradation as shown previously [12]. Therefore, the fast second-dimension separation at high temperature is unfavorable for AAE resolution.

3.1. Rt-γDEXsa/RTx-1701 column set

Initially, a 2-m midpolarity 14% cyanopropylphenyl/86% dimethyl polysiloxane RTx-1701 capillary column served as the second-dimension column. A characteristic chromatogram of the master standard obtained under optimized temperature program (method A, Table 1) is shown in Fig. 1. The RTx-1701 column compensated for the lack of selectivity of the Rt-γDEXsa for L-Thr/L-Asp and L-Ser/D-Met, respectively, and allowed their baseline resolution in the second-dimension. However, L-Leu and D-Ile still coeluted. MCF-Phe enantiomers were not resolved at all by the chiral Rt-γDEXsa column and, therefore, could not be separated by the RTx-1701 column either.

3.2. Rt-γDEXsa/ZB-AAA column set

Previously, Kaspar et al. had demonstrated the successful separation of Leu and Ile as their propyl chloroformate (PCF) derivatives on a 15-m ZB-AAA capillary column that reportedly consists of 50% phenyl/50% dimethyl polysiloxane [19,20]. Therefore, the ZB-AAA column was tested next as second-dimension column. A representative chromatogram of the master mixture obtained with a temperature program (method B, Table 1) comparable to the recently optimized GC–qMS method [12] is pictured in Fig. 2. Again L-Thr/L-Asp and L-Ser/D-Met, which coeluted from the chiral column, were resolved completely in the second-dimension. In addition, partial resolution of D-Ile and L-Leu was observed. Following optimization of the temperature program (method C, Table 1), baseline separation was achieved for all analytes except for the Phe enantiomers. This is demonstrated by first and second-dimension retention times in Table 2 and by a 2D chromatogram of the master standard in Fig. 3A as compared to a respective measurement in 1D mode (Fig. 3B). The 1D GC–TOFMS measurement yielded 4 unresolved peak pairs using GC method C (Table 1), reflecting the insufficient selectivity of the Rt-γDEXsa column. Selectivity was improved by using thermal modulation and the orthogonal separation properties of the second-dimension ZB-AAA column. Enhanced

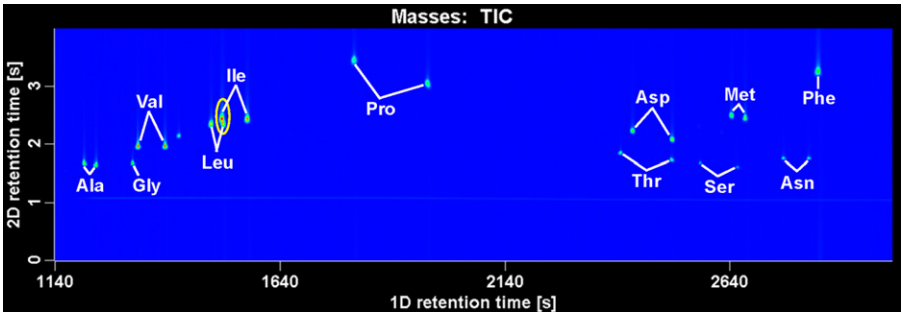

Fig. 2. Total ion current 2D chromatogram of the master mixture using the Rt-γDEXsa/ZB-AAA column set and GC method B. D-Ile/L-Leu isomers are encircled.

Table 2
First and second-dimension retention times and fragment ion masses used for quantification of the MeOH/MCF AAE-derivatives by GC × GC–TOFMS (method C, Table 1).

AA	1st dimension retention time (s)	2nd dimension retention time (s)	Quantifier analyte + U-^{13}C, U-^{15}N-labeled internal standard (*m/z*)
D-Ala	1916	2.11	102 + 105
L-Ala	1976	2.11	102 + 105
Gly	2172	2.25	88 + 90
D-Val	2180	2.90	130 + 135
L-Val	2372	2.89	130 + 135
D-Leu	2572	3.81	144 + 150
L-Leu	2660	3.26	144 + 150
D-Ile	2648	3.53	144 + 150
L-Ile	2764	2.48	144 + 150
D-Pro	3004	3.45	128 + 133
L-Pro	3176	2.66	128 + 133
D-Thr	3512	1.71	147 + 149
L-Thr	3592	1.62	147 + 149
D-Asp	3536	2.00	160 + 164
L-Asp	3596	1.89	160 + 164
D-Ser	3644	1.61	118 + 121
L-Ser	3712	1.61	118 + 121
D-Met	3708	2.46	162 + 167
L-Met	3740	2.46	162 + 167
D-Asn	3812	1.77	127 + 132
L-Asn	3864	1.77	127 + 132
D + L-Phe	3900	3.28	162 + 171

resolution of enantiomers that were separated by a temperature program on the chiral first-dimension column was achieved due to the fast and therewith approximately isothermal separation on the second-dimension column. It allows additional separation of enantiomers even though the second-dimension selector provides no stereo-specific retardation. This can be seen for the enantiomers of Leu, Ile, and Pro in Fig. 3A.

3.3. Quantification and method validation

Calibration curves were generated for absolute quantification of AAEs. Table 2 lists fragment ion masses chosen for quantification. Values for linear range, R^2 and reproducibility are shown in Table 3. For direct comparison, Table 3 also includes the values obtained for 1D-GC–qMS. GC × GC–TOFMS calibration curves were linear with the square values of the sample correlation coefficient R ranging between 0.9938 and 0.9992, which is comparable, albeit inferior to the 1D method, whose R^2 values ranged from 0.9956 to 1.0000. Lower limits of quantification (LLOQ) were in the range of 0.03–2 μM. Octaplicate analysis of a serum specimen yielded relative standard deviations (RSDs) below 5% except for D-Ala (12.2%), D-Asp (16.6%), and D-Asn (9.9%), whereas hexaplicate 1D-GC–qMS analysis yielded in general RSDs < 4%. For evaluation of method accuracy, 48 urine and 43 serum specimens were analyzed by both GC × GC–TOFMS and the 1D-GC–qMS method that had been validated previously by comparison to an established non-chiral GC–qMS method for quantitative AA analysis [12]. Determined D + L amounts of free AAs had been compared by averaged recoveries. Here, mean recoveries were calculated using the data generated by chiral 1D-GC–qMS as reference. Mean recoveries, mean deviations as results of the Bland–Altman plots, and Pearson correlation coefficients are shown in Table 4. Only analytes detected in $n \geq 20$ urine and serum specimens, respectively, were evaluated. Mean recoveries between 80% and 120% and mean deviations below 15% were defined as quality criteria for the accuracy. These criteria were fulfilled for both enantiomers of Ala, Ser, and Asn, as well as for Gly, L-Val, L-Pro, L-Asp, L-Met, and D + L-Phe in the analysis of urine. Urinary concentrations of D-Val and D-Met were below the LLOQ for either method in most of the investigated specimens. GC × GC–TOFMS yielded slightly higher (mean deviation of 18%) urinary L-Ile concentrations. Nevertheless, both mean recovery (114.5%) and the correlation coefficient (R = 0.996) between the methods were excellent. Compared to 1D-GC–qMS, GC × GC–TOFMS gave slightly lower urinary concentrations for L-Thr and D-Asp with mean deviations of 21.1% and 21.4%, respectively, whereas mean recoveries were 93.3% and 81.6%. Note that superior concordance was observed for L-Met (mean deviation of 0.2%) despite a low correlation coefficient of 0.913. For D-Thr, a method comparison was not possible, because a highly abundant urinary matrix compound had interfered with its 1D-GC–qMS analysis. The low values of concordance observed for D-Leu, D-Pro, and

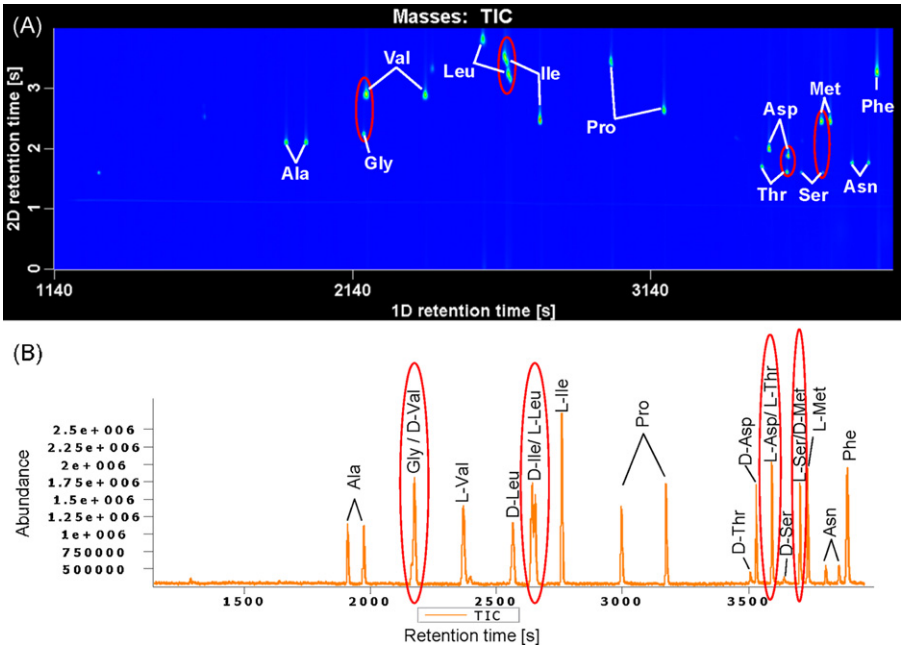

Fig. 3. Total ion current chromatograms of the master mixture recorded in (A) 2D and (B) 1D mode using Rt-γDEXsa/ZB-AAA column set and method C. Analytes coeluting from the Rt-γDEXsa column are encircled in both chromatograms.

Table 3
Comparison of linear ranges, R^2 values and relative standard deviations (RSDs) for AAE analysis in serum by GC × GC–TOFMS and GC–qMS.

AA	GC × GC–TOFMS			GC–qMS		
	Linear range (μM)	R^2	RSD (%; $n = 8$)	Linear range (μM)	R^2	RSD (%; $n = 6$)
D-Ala	0.031–1000	0.9971	12.15	0.031–500	0.9998	1.10
L-Ala	0.061–1000	0.9974	2.16	0.122–500	0.9996	0.95
Gly	0.031[a]–1000	0.9979	3.78	0.977–500	0.9996	0.87
D-Val	0.244–500	0.9971	–	0.244–500	0.9999	–
L-Val	0.061[a]–500	0.9961	3.81	0.244–500	0.9999	0.81
D-Leu	0.244–1000	0.9974	–	0.244–500	1.0000	–
L-Leu	0.061–1000	0.9954	1.28	–	–	–
D-Ile	0.061–1000	0.9970	–	–	–	–
L-Ile	0.061–1000	0.9973	3.07	0.061–500	0.9998	0.87
D-Pro	0.031–500	0.9988	4.52	0.061–500	0.9998	1.31
L-Pro	0.061–500	0.9970	3.38	0.061–500	0.9999	0.73
D-Thr	0.122[a]–500	0.9986	–	0.977–1000	0.9996	–
L-Thr	0.061[a]–500	0.9980	3.53	1.953–1000	0.9988	1.62
D-Asp	0.031[a]–1000	0.9938	16.64	0.122–500	0.9998	3.87
L-Asp	0.061[a]–1000	0.9990	3.18	0.977–500	0.9994	0.70
D-Ser	0.244[a]–1000	0.9987	–	1.953–1000	0.9999	–
L-Ser	0.031[a]–1000	0.9991	2.37	31.25–1000	0.9956	–
D-Met	1.953–1000	0.9988	–	0.488–1000	0.9999	–
L-Met	0.977–1000	0.9992	2.56	0.244–1000	0.9996	1.06
D-Asn	0.061[a]–1000	0.9973	9.93	0.244–1000	0.9999	–
L-Asn	0.031[a]–1000	0.9983	3.43	0.244–1000	0.9999	1.02
DL-Phe	0.061–1000	0.9978	3.41	0.061–1000	0.9995	1.13

[a] At least two additional calibration points were included at the lower end of the GC × GC calibration curve compared to the GC–qMS calibration curve.

D-Asp resulted from urinary levels close to the respective LLOQs of either method, and in the case of D-Pro and D-Asp due to insufficient LLOQs for the GC–qMS method.

Similar results were obtained for the analysis of serum. Accuracy was high for both enantiomers of Ala and Pro, and for Gly, L-Val, L-Asp, L-Met, L-Asn, and D + L-Phe. In Fig. 4A and B, Bland–Altman plots demonstrate good agreement between GC–qMS and GC × GC–TOFMS for the serum levels of L-Ala and D-Pro. Serum levels of D-Val, D-Leu, D-Thr, D-Asp, and D-Met in most of the analyzed specimens were below LLOQ for either method. Again a slight overestimation of L-Ile (129.4%) by GC × GC–TOFMS was observed. Bland–Altman plots of L-Thr and L-Ile serum analysis displayed in Fig. 4C and D picture exemplary low concordances with the reference GC–qMS method. The plots show a proportional error and can be classified as Bland–Altman plot types D and E, respectively, as recently defined by Kaspar et al. [17]. Type D describes increasingly positive differences at high concentrations whereas type E describes increasingly negative differences. Apparently lower L-Thr amounts determined by GC × GC–TOFMS result from L-Thr overquantification by GC–qMS analysis that was affected by a coeluting serum compound, which appeared at elevated levels in serum specimens of one patient and resulted in the 7 outliers visible in Fig. 4D. Systematically lower L-Ser concentrations were found by GC × GC–TOFMS for concentrations below 330 μM for both urine and serum, whereas concentrations above 330 μM determined in urine were systematically increased. A flat calibration curve of the GC–qMS method with a high *y*-axis interception caused by overlapping D-Met, and a serum matrix peak are responsible for this trend. The GC × GC approach provides more reliable L-Thr and L-Ser results as matrix compounds were separated from targets in the second-dimension. However, their accuracy could not be ascertained because of the lack of both a validated refer-

Table 4
Comparison of quantitative AAE data obtained by a validated chiral GC–qMS method and the GC × GC–TOFMS method. Mean recoveries, mean deviations, and Pearson correlation coefficients are shown for all analytes whose urine and serum concentrations, respectively, fell within the linear ranges of both methods for $n \geq 20$ specimens.

AA	Urine				Serum			
	n	Mean recovery (%)	Mean deviation (%)	*R*	*n*	Mean recovery (%)	Mean deviation (%)	*R*
D-Ala	48	93.9	3.8	0.989	43	90.3	12.0	0.975
L-Ala	48	101.3	1.8	0.994	43	104.4	4.2	0.907
Gly	47	101.9	1.1	0.998	41	104.8	4.5	0.996
D-Val	<20	–	–	–	<20	–	–	–
L-Val	48	105.6	5.6	0.994	43	111.1	10.6	0.916
D-Leu	47	78.4	17.6	0.970	<20	–	–	–
L-Ile	48	114.5	18.5	0.996	43	129.4	25.4	0.991
D-Pro	25	116.4	22.1	0.819	34	91.3	11.2	0.987
L-Pro	48	101.7	5.9	0.993	42	114.8	12.6	0.957
D-Thr	–[a]	–[a]	–[a]	–[a]	<20	–	–	–
L-Thr	48	93.3	21.1	0.982	43	72.2	44.1	0.369
D-Asp	45	81.6	21.4	0.919	<20	–	–	–
L-Asp	45	84.2	10.6	0.989	43	115.6	15.0	0.994
D-Ser	48	89.8	5.2	0.977	–[a]	–[a]	–[a]	–[a]
L-Ser	34	81.5	8.8	0.991	42	74.7	29.1	0.873
D-Met	<20	–	–	–	<20	–	–	–
L-Met	44	111.9	0.2	0.913	42	101.2	0.2	0.970
D-Asn	48	85.8	10.3	0.988	–[a]	–[a]	–[a]	–[a]
L-Asn	48	100.9	4.9	0.999	43	103.1	3.4	0.984
D + L-Phe	48	105.1	8.0	0.998	43	103.3	2.9	0.967

[a] Analyte was affected by matrix overlaps that impeded accurate quantification.

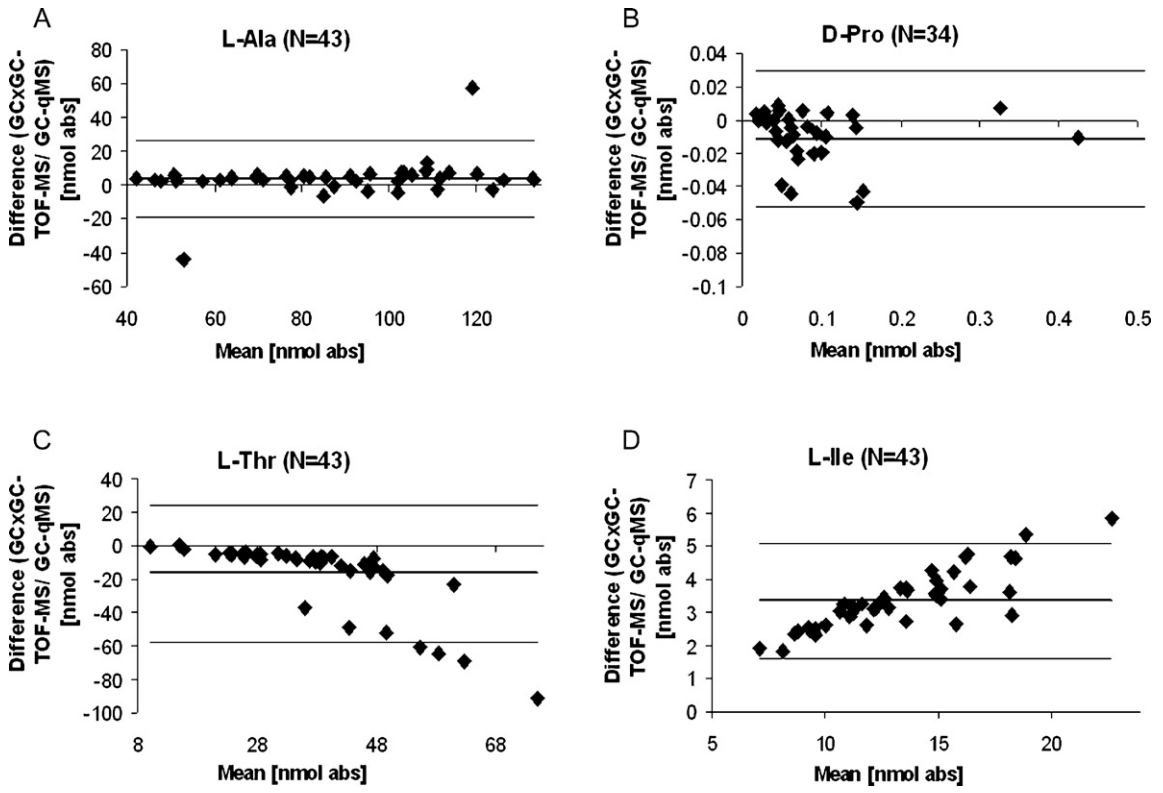

Fig. 4. Bland–Altman plots for the analysis of (A) L-Ala and (B) D-Pro in serum show good agreement between GC–qMS and GC × GC, while the Bland–Altman plots for (C) L-Thr and (D) L-Ile show proportional error in agreement between the two methods.

ence method and a certified standard for Ser and Thr enantiomers. Furthermore, a serum matrix peak interfered with the quantification of D-Ser using both 1D and 2D GC. Finally, a coeluting serum matrix compound impeded GC–qMS analysis of D-Asn, but the adequately resolved GC × GC peak and accurate urine analysis indicate accuracy of D-Asn serum analysis.

3.4. Application to serum specimens from patients with liver cirrhosis

An exemplary application of GC × GC–TOFMS to diagnostics was performed by analyzing serum specimens from $n = 16$ healthy probands and $n = 25$ patients with liver cirrhosis. The clear trend of increased serum levels of D-AAs in liver cirrhosis patients is visible in Fig. 5A. Only D-Asp concentrations were not increased compared to the respective mean concentration of the control group. D-Val, D-Leu, and D-Thr were found above the LLOQ only in some of the serum specimens of cirrhosis patients. D-Ile and D-Met were detected in none of the samples, and D-Ser could not be measured because of the interference by a serum matrix compound as mentioned above. Compared to the controls, significantly elevated serum concentrations of D-Pro ($P = 0.013$) and D-Ala ($P = 0.00008$) were observed as determined by a two-tailed Student's t-test. Mean D-Asn concentrations were not tested because of an insufficient number ($n = 2$) of values above LLOQ in the control group. Determined concentrations of D-Ala, D-Pro and D-Asn + D-Asp in control sera were in good agreement with respective serum levels reported previously for healthy volunteers [21,22]. L-AA serum levels were significantly decreased in liver cirrhosis specimens as shown in Fig. 5B: L-Ala ($P = 0.0051$), L-Ile ($P = 0.036$), L-Ser ($P = 0.0099$), L-Asn ($P = 0.0011$), L-Val ($P = 0.00028$), and L-Leu ($P = 0.0003$). The increased D-AA serum levels observed for liver cirrhosis reflect the

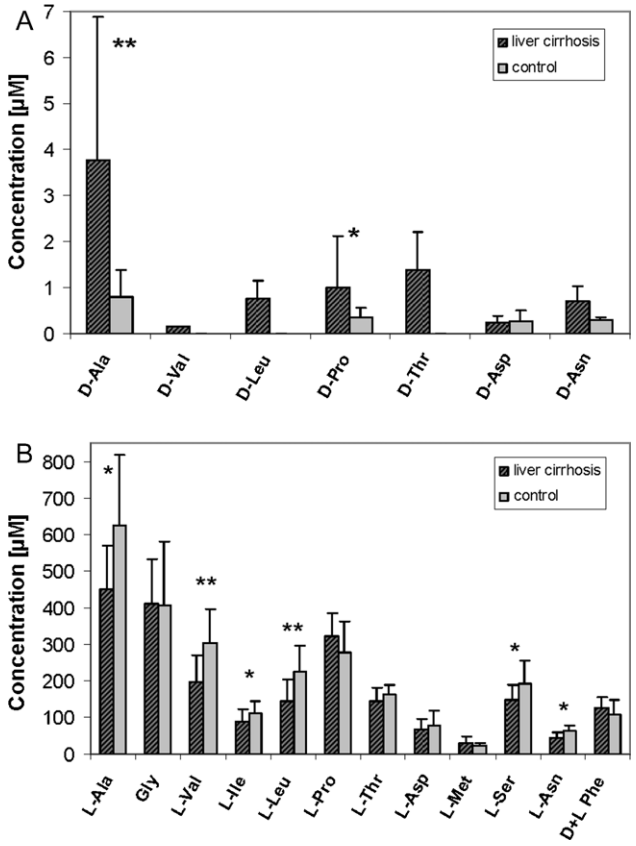

Fig. 5. Mean concentrations and SDs of (A) D-AAs and (B) L-AAs in serum specimens of $n = 25$ patients suffering from liver cirrhosis compared to the respective values of $n = 16$ healthy probands (*$P < 0.05$, **$P < 0.001$).

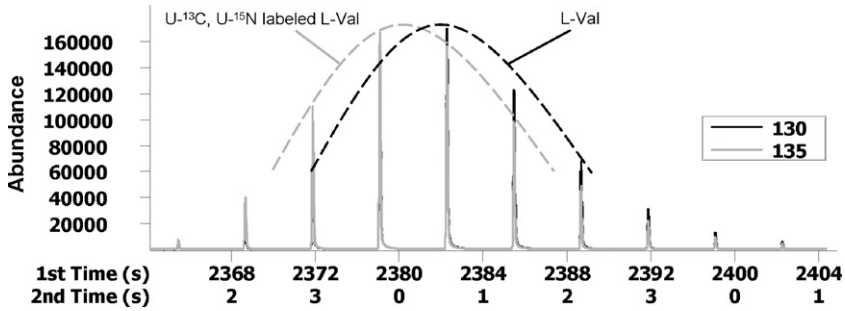

Fig. 6. Extracted ion chromatogram of L-Val quantification masses. Peak envelopes (dashed lines) of L-Val and U-^{13}C, U-^{15}N labeled L-Val are indicated to demonstrate their position shift and the varying analyte-to-internal standard area ratio for each fraction.

loss of intact liver parenchyma and, hence, a reduced enzymatic capacity to catalyze D-AA decomposition.

3.5. Comparison of GC–qMS with GC × GC–TOFMS

The quantification parameters determined for GC × GC–TOFMS and GC–qMS are shown in Table 3. Linear ranges, square values of the sample correlation coefficient R, and relative standard deviations (RSD) for replicate AAE analysis of a serum sample ($n = 8$) are compared. Limits of detection (LOD) are not given, because the internal standard mix contained up to 2% unlabeled AAs that appeared as blank values in the chromatograms as reported recently [12]. Since blank values affect LODs, this parameter was not considered for method comparison. GC × GC–TOFMS yielded distinctly lower LLOQs for Gly, L-Val, and both enantiomers of Thr, Asp, Ser, and Asn. Chromatographic band focusing in the thermal modulator and fast second-dimension separation yield narrow peaks and, thus, enhance detection sensitivity [13]. Analytes eluting late from the chiral column showed an improved LLOQ in GC × GC–TOFMS, because column bleeding in contrast to GC–qMS was separated from all analytes in the second-dimension. Linearity of calibration curves was good for both methods.

Peak resolution was improved by coupling two columns with orthogonal separation characteristics. All target analytes were resolved adequately from matrix peaks except for D-Ser in serum, whereas D-Asn and both enantiomers of Thr and Ser were disturbed by matrix compounds in GC–qMS analysis. Separation of D-Met/L-Ser and L-Thr/L-Asp, respectively, which had coeluted from the chiral column, was accomplished with the GC × GC approach [12]. Separation of D-Ile/L-Leu was possible but required decreased operation temperatures for both columns and, as a consequence, increased analysis time from 44 to 66 min.

Analysis time of 2D data took also longer. Automatic peak assignment by comparison of found mass spectra with given standard spectra was sometimes incorrect, such as for D-Val and Gly that dissociated into similar ions and featured almost identical first-dimension retention times. Another problem resulted from the slightly earlier elution of internal standards compared to the respective analytes as shown in Fig. 6. Since the base fraction peak of the labeled AA appeared one modulation before the analyte maximum, the analyte-to-standard area ratio was different for each fraction. Thus, peaks from all modulations had to be integrated to determine the response. As the software mostly integrated the major analyte fractions, the remaining fractions had to be integrated manually and summed up, leading to a significant increase in data analysis time, as highly abundant L-AAs and internal standards may yield ten and more modulations (visible in Fig. 6). These problems reflect the complexity of GC × GC–TOFMS data handling, because more parameters including a mass spectral match factor need to be considered in combining all modulated peaks. Due to the impact of noise, low abundant modulated peaks suffer from an insufficient spectral match and, therefore, are not integrated automatically. Reproducible manual inclusion of a great number of sub-fraction integrals is a challenging task and contributes to higher RSDs for GC × GC–TOFMS quantitative data as compared to the excellent repeatability of chiral GC–qMS analysis (RSDs < 4%). In this study, a large sample volume (150 μL) was derivatized and extracted and splitless injection was used to increase intentionally peak intensities in an effort to facilitate detection of D-AAs. As a consequence, we observed broad peaks, peak tailing, and in turn a great number of modulations for L-AAs and stable isotope-labeled internal standards. Optimally, each first-dimension peak should be sampled three to five times, which was the case for D-AAs. The correction of the area integral of a D-AA with a stable isotope-labeled L-AA that generates ten or more modulations is not optimum and, consequently, lowers repeatability of D-AA quantification results as reflected in comparatively great RSDs for D-Asp (16.6%), D-Ala (12.2%), and D-Asn (9.9%), whereas RSDs for the other target analytes were <5%. Comparable peak tailing was observed for L-AAs and internal standards, whereas it was barely visible for D-AAs. This also indicates that correction of area integrals of D-AAs by labeled L-AAs is unfavorable as the differences in concentration may be as great as three orders of magnitude. A set of stable isotope-labeled D-AAs for D-AA area integral correction would probably improve precision of quantification results, but is not available at present.

The same number of AA types eluted from the Rt-γDEXsa column in GC × GC analysis as in GC–qMS analysis. Reasons for the failure to detect the proteinogenic AAs Glu, Gln, Cys, Lys, His, Arg, Tyr, and Trp remain to be elucidated, but may be due to chemical or thermal derivative instability as reported for propyl chloroformate derivatized arginine [19], or strong interactions with the CD core leading to strong retardation and broad peaks that vanish into the baseline. Anyway, the presented GC × GC approach bears the potential to be expanded to enantiomers of other small organic acids due to higher peak capacity compared to 1D GC separation. Enantiomers of lactic acid and 3-methyl-2-oxo-valeric acid were found to be perfectly resolved in the chromatogram of a serum sample (data not shown). They were identified by searching for equal mass spectra and their comparison to fragmentation spectra of analyzed standards. Additional peak pairs exhibiting similar mass spectra await identification in serum. Inclusion of these chiral compounds in an expanded analysis will require further method optimization to ensure baseline resolution and accurate quantification of all target enantiomers.

3.6. Comparison of chiral GC × GC–TOFMS to published methods

Recently, we reported the superior performance of the GC–qMS method over other published methods for the quantitative analysis of AAEs in physiological fluids [12]. No other 1D GC method had been reported to quantify more than 5 D-AAs in serum

and urine without pre-separation of AAs from biological matrix compounds [12]. To date, Nagata et al. had presented the best quantitative 1D-LC method that allowed the baseline resolution of 12 pairs of AAEs; however, due to poor sensitivity (LODs ranged from 4 to 10 μM), only 3 D-AAs were detected in blood plasma [23]. Two-dimensional HPLC performed by Hamase et al. yielded comparable sensitivity to GC–qMS and GC × GC–TOFMS analysis with LOQs of 0.25 μM. The method enabled direct quantification of 4 D-AAs in physiological fluids [24]. Consequently, the optimized GC × GC–TOFMS method presented here for the determination of AAEs in physiological fluids is at present to the best of our knowledge the most effective technique for AAE analysis, enabling quantification of 8 D-AAs in serum or urine in a single chromatographic run.

4. Conclusions

Comprehensive GC × GC–TOFMS was applied successfully to the quantitative AAE analysis in serum and urine. Coupling of a γ-CD column (Rt-γDEXsa) and an AA selective ZB-AAA column yielded baseline separation of 20 MCF-derivatized AAEs within 66 min under optimized temperature program conditions. Comparison to a recently published chiral GC–qMS method revealed that the GC × GC approach excelled in detection sensitivity and resolution, which were essential for D-AA trace recognition in the presence of an L-AA excess. GC × GC–TOFMS yielded distinctly lower LLOQs for 10 AAEs as compared to single ion monitoring by quadrupole MS. All target analytes were separated adequately, from serum matrix peaks using GC × GC–TOFMS with the exception of D-Ser. In contrast, GC–qMS, which was overall faster and more reliable, failed to resolve D-Thr, L-Thr, D-Asn, D-Ser, and L-Ser from urine and serum matrix compounds, while D-Ile, L-Thr, and L-Ser could not be separated from L-Leu, L-Asp, and D-Met, respectively, using the γ-CD column as the only dimension. However, they were baseline resolved by the second-dimension column in GC × GC analysis. Neither technique distinguished the Phe enantiomers. A further advantage of GC × GC analysis is its outstanding peak capacity that promises expansion of the method to additional enantiomers of biomedical relevance, such as lactic acid and other small organic acids [25].

Acknowledgments

This project was funded in part by BayGene and the intramural ReForM program. We thank Drs. Ernst Holler, Karin Landfried, and Claus Hellerbrand for providing serum and urine specimens, and Inka Appel for her help in searching the spectra for additional enantiomers.

References

[1] M. Friedman, Chem. Biodivers. 7 (2010) 1491.
[2] M. Friedman, J. Agric. Food Chem. 47 (1999) 3457.
[3] H. Brückner, M. Hausch, Chromatographia 28 (1989) 487.
[4] H. Brückner, M. Hausch, Amino Acids. Chemistry, Biology and Medicine, Escom, Leiden, 1990, p. 1172.
[5] H. Brückner, M. Hausch, Milchwissenschaft 45 (1990) 357.
[6] H. Zahradnickova, P. Husek, P. Simek, P. Hartvich, B. Marsalek, I. Holoubek, Anal. Bioanal. Chem. 388 (2007) 1815.
[7] R. Pätzold, A. Schieber, H. Brückner, Biomed. Chromatogr. 19 (2005) 466.
[8] H.S.M. Ali, R. Pätzold, H. Brückner, Amino Acids 38 (2010) 951.
[9] A. D'Aniello, G. D'Onofrio, M. Pischetola, G. D'Aniello, A. Vetere, L. Petrucelli, G.H. Fisher, J. Biol. Chem. 268 (1993) 26941.
[10] M. Pilone, Cell. Mol. Life Sci. 57 (2000) 1732.
[11] M.C. Waldhier, M.A. Gruber, K. Dettmer, P.J. Oefner, Anal. Bioanal. Chem. 394 (2009) 695.
[12] M.C. Waldhier, K. Dettmer, M.A. Gruber, P.J. Oefner, J. Chromatogr. B: Analyt. Technol. Biomed. Life Sci. 878 (2010) 1103.
[13] A. Lee, K. Bartle, A. Lewis, Anal. Chem. 73 (2001) 1330.
[14] L. Mondello, P. Tranchida, P. Dugo, G. Dugo, Mass Spectrom. Rev. 27 (2008) 101.
[15] M. Junge, H. Huegel, P.J. Marriott, Chirality 19 (2007) 228.
[16] J. Bland, D. Altman, Lancet 1 (1986) 307.
[17] H. Kaspar, K. Dettmer, Q. Chan, S. Daniels, S. Nimkar, M. Daviglus, J. Stamler, P. Elliott, P. Oefner, J. Chromatogr. B: Analyt. Technol. Biomed. Life Sci. 877 (2009) 1838.
[18] K. Dettmer, M. Almstetter, I. Appel, N. Nürnberger, G. Schlamberger, W. Gronwald, H. Meyer, P. Oefner, Electrophoresis 31 (2010) 2365.
[19] H. Kaspar, K. Dettmer, W. Gronwald, P. Oefner, J. Chromatogr. B: Analyt. Technol. Biomed. Life Sci. 870 (2008) 222.
[20] C. Cipollina, A. Ten Pierick, A.B. Canelas, R.M. Seifar, A.J.A. Van Maris, J.C. Van Dam, J.J. Heijnen, J. Chromatogr. B: Analyt. Technol. Biomed. Life Sci. 877 (2009) 3231.
[21] H. Brückner, A. Schieber, Biomed. Chromatogr. 15 (2001) 166.
[22] D.W. Armstrong, M. Gasper, S.H. Lee, J. Zukowski, N. Ercal, Chirality 5 (1993) 375.
[23] Y. Nagata, R. Masui, T. Akino, Experientia 48 (1992) 986–988.
[24] K. Hamase, A. Morikawa, T. Ohgusu, W. Lindner, K. Zaitsu, J. Chromatogr. A 1143 (2007) 105.
[25] M. Heil, F. Podebrad, T. Beck, A. Mosandl, A. Sewell, H. Böhles, J. Chromatogr. B: Analyt. Technol. Biomed. Life Sci. 714 (1998) 119.